Published online: December 30, 2019

Original Research

Baicalin attenuated substantia nigra neuronal apoptosis in Parkinson's disease rats via the mTOR/AKT/GSK-3β pathway

Heng Zhai , Zihua Kang *, Haibo Zhang , Junjie Ma and Guangxin Chen

Emergency Department, Central Hospital of Zibo, Zibo 255000, P. R. China

*Correspondence: kangzihuakk@163.com (Zihua Kang)

DOI:10.31083/j.jin.2019.04.192

This focus of our research is to investigate the protective effect of Baicalin on apoptosis and mTOR/AKT/GSK-3β pathway in substantia nigra neurons in a rat model for Parkinson's disease, induced by 6-Hydroxydopamine. Thirty healthy female Sprague-Dawley rats were randomly divided into control group, model group, and Baicalin group. The Parkinson model was established by injecting 6-Hydroxydopamine into the right substantia nigra of rats in model and Baicalin group. The rats in Baicalin group were intragastrically administered with Baicalin (25 mg/kg/day) for four weeks. At the same time, the rats in control and model groups were intragastrically administered with equivalent solvents. We observed the rat turns, rotation speed and left forelimb usage. The protein expression levels of α-SYN, mTOR, AKT, and GSK-3β in substantia nigra were detected by immunohistochemistry and Western blotting. Compared with model group, Baicalin significantly reduced the number of rotation speeds and neuron apoptosis ($P < 0.001$, respectively). However, the left forelimb use rate was notably increased after treatment with Baicalin ($P < 0.001$, respectively). Also, Baicalin decreased the expression levels of α-SYN, mTOR, AKT, and GSK-3β in rats when compared with those in model group ($P < 0.001$, respectively).

Keywords

Baicalin; 6-Hydroxydopamine; Parkinson's disease; mTOR/AKT/GSK-3β pathway; rat model

1. Introduction

Parkinson's disease (PD) is most commonly detected in elderly populations. It is characterized by a decrease in nigrostriatal dopaminergic (DA) neurons, presenting as its main clinical symptoms- tremors, myotonia, and movement disorders(Lazzarini et al., 2013). As such, there is a great need for experimental models to enhance our understanding of the etiology of PD and expand the currently limited set of treatment options. A range of animal models of PD is currently in use, including neurotoxin-based approaches (e.g. exposure of rodents or non-human primates to 6-OHDA, MPTP, or agrochemicals) and gene-based approaches (e.g., transgenic or viral vector-mediated models) (Konnova et al., 2018). The 6-OHDA-induced rat model is known to be stable, reliable, reproducible, and consistent with the pathogenesis and clinical characteristics of PD (Deng et al., 2017; Thiele et al., 2012).

Previous studies have reported the central role of the mTOR/AKT pathway in cell apoptosis (Heras-Sandoval et al., 2014; Prusiner et al., 2015; Sadowski et al., 2015). Several nervous system diseases result from dysregulated AKT expression (Chung et al., 2011). Specifically, AKT phosphorylation was found to be significantly reduced in substantia nigra of PD patients (Heras-Sandoval et al., 2014). GSK-3β, an important gene target downstream of AKT, is a crucial regulator of cell proliferation and apoptosis (Khwanraj et al., 2016). p-GSK-3β expression was also significantly reduced in PD mouse models, suggesting a key role of AKT and GSK-3β in the development of PD (Morales-García et al., 2013).

Dopamine replacement drugs are commonly used in clinical practice to ameliorate the symptoms of PD (Radder et al., 2017). However, after long-term use, patients are prone to various adverse reactions, such as switch phenomenon, mental symptoms, and dyskinesia. Baicalin (BAI) is a polyphenol hydroxyl flavone monomer extracted from *Scutellaria baicalensis*. BAI displays various biological effects, including bacteriostasis, antitumor functions, and inhibition of cell apoptosis (Jiang et al., 2018; Shou et al., 2017; Tan et al., 2012; Yang et al., 2014). We hypothesize that BAI will also improve nerve cell apoptosis induced by PD. This study evaluates the effect of BAI on PD-induced nerve injury, to explore its potential use as a therapeutic intervention against PD.

2. Materials and methods

2.1 Chemicals and antibodies

BAI was obtained from Shandong Sanjing Pharmaceutical Co., Ltd (Shandong, China). 6-OHDA and apomorphine were purchased from Sigma Chemical Co. (St.Louis, MO, USA). Chloral hydrate solution was obtained from Shanghai JINSUI Bio-Technology Co., Ltd (Shanghai, China). Penicillin was purchased from Harbin Pharmaceutical group holding Co., Ltd (Harbin, China). The following antibodies were purchased from Abcam Technology (Cambridge, UK) and applied at the concentrations described: anti-p-mTOR (S2448) (1 μg/mL), anti-mTOR (1 : 2000), anti-α-SYN, anti-p-AKT (T308) (1 : 1000), anti-AKT

(EPR16798) (1 : 10,000), anti-GAPDH (reduced glyceraldehyde-phosphate dehydrogenase) (1 : 10,000), anti-p-GSK-3β (Y216) (1 : 1000), and anti-GSK-3β (1 : 2000). Secondary goat anti-rabbit and -mouse IgG, and mouse anti-goat antibodies were purchased from ZSGB Biotech Co., Ltd. (Beijing, China). Unless specified, all other reagents are obtained from Sigma Chemical Co. (St. Louis, MO, USA).

2.2 Animal protocols and PD rat model

All experimental procedures were conducted in accordance with Chinese legislation and US National Institutes of Health (NIH) guidelines for the use and care of experimental animals. Animal experiments were approved by the institutional ethics committee of Henan University of Science and Technology (No. EDCH2015011201). Thirty adult female SD (Sprague-Dawley) rats (180 $\pm$ 20 g) were purchased from the First Affiliated Hospital and College of Clinical Medicine of Henan University of Science and Technology. Rats were housed in a standard laboratory animal room, maintained at 20-25 °C and 60% relative humidity with standard management conditions of 12 h light/dark cycle. Rats were fed adaptively for one week.

The PD model was established as previously described, with minor modifications (Schwarting et al., 1991). The rats were anesthetized by intraperitoneal injection of 10% chloral hydrate solution (5 mL/kg, chloral hydrate 0.5 g/kg), and top hair was removed. The rats were fixed in SN-2 type brain stereotaxis. Following disinfection, the skin and fascia were opened, and the skull exposed. The raphe nucleus was located based on the rat brain atlas. Coordinates selected on the right substantia nigra were as follows: incisor line below the level of the line -3.3mm, A/P (before 4.8 mm, L/R halogen Center) (from the center around 1.6 mm, O/V halogen) (from the meningeal surface depth) 8.2 mm. After locating the right side of the substantia nigra, the right skull was drilled. Six μL of freshly prepared 6-OHDA (2 μg/L) was slowly administered with a microinjector at a rate of 1 μL/min for 3 minutes. The needle was slowly retracted at a rate of 1 mm/min. After the injection, the skin was sutured and disinfected with iodine. Rats were intraperitoneally injected with penicillin (1×10^5 U/kg) every day, and local wounds were disinfected with iodine. Sutures were removed under anesthesia after seven days. Two weeks after the operation, rats were intraperitoneally injected with 1 mL 0.01% apomorphine.

Following surgery, rats were monitored for the number of rotations to the healthy side every 5 min and the total number of rotations within 40 min. Measurements were performed and recorded once a week. A rotation time of $\geq$ 7 circles/min was scored as a positive result. Rats that scored positive for four weeks were classified as successful PD model rats. The 20 successful PD model rats were randomly divided into two groups: model and BAI. The ten rats left untreated were classified as the normal control (NC) group.

Rats in the NC and model groups were gavaged with 0.9% normal saline, while BAI group rats were gavaged with BAI solution (25 mg/kg). Bodyweight was measured once per week. After feeding for four weeks, rats were sacrificed by cervical dislocation after terminal anesthesia via intraperitoneal injection of 50 mg/kg pentobarbital. When the rats stopped breathing, the thoracic cavity was opened, and the heart was exposed. Blood was removed from the left ventricular intubation by PBS perfusion. The brain tissue was removed and fixed in 10% paraformaldehyde for 4-6 hours until use.

2.3 Behavioral test

After feeding for four weeks, rat rotation behavior was measured as previously described (Tang et al., 2017). The left forelimb use rate was measured using the cylinder test (Schallert et al., 2000). Briefly, the number of times that the rats' left and/or right forelimbs touched the wall within 5 min was observed and recorded. Left forelimb use rate = (Left time + 0.5 $\times$ bilateral times) / (Right time + Left times + Bilateral times) $\times$ 100%.

2.4 TUNEL assay

Apoptosis of rat nerve cells was detected by Terminal Deoxynucleotidyl Transferase dUTP Nick End Labeling (TUNEL) assay (Huang et al., 2019). Briefly, brain tissues were dehydrated, embedded in paraffin, and sliced into five μm sections. TUNEL assay was performed on sections using a TUNEL kit (Roche, USA) in accordance with manufacturer's instructions. Staining was observed under the Olympus Bx41 inverted microscope. TUNEL-stained dark brown cell number was quantified as described.

2.5 Immunohistochemistry (IHC) assay

The expression level of mTOR, p-mTOR, AKT, p-AKT, GSK-3β and p-GSK-3β proteins in rat brain tissue was measured by IHC (Saxena et al., 2016; Sun et al., 2019). Briefly, sections of brain tissue were dewaxed and rehydrated. Endogenous peroxidase activity was eliminated by incubating sections in 3% H_2O_2. Subsequently, sections were incubated in 1% goat serum (diluted with PBS) for 60 min, following which primary antibodies were applied overnight at 4 °C. Horseradish peroxidase (HRP) secondary antibody was applied at room temperature for one h, and the signal was developed with DAB (3,3'-Diaminobenzidine) chromogen according to the manufacturer's specifications. The specificity of staining was confirmed using matched isotype control antibodies. All sections were counterstained with hematoxylin. Staining was examined and imaged using a light microscope and Image-Pro Plus 6.0 Image analysis software.

2.6 Western blotting assay

Proteins were extracted by homogenizing whole brain tissues in cold RIPA buffer (Beyotime Institute of Biotechnology, Shanghai, China). The total protein was centrifuged at 13,000 $\times$ g for 4 min at 4 °C. The supernatants were collected, and protein concentration measured using a modified BCA (bicinchoninic acid) protein concentration assay kit (Beyotime Institute of Biotechnology, Shanghai, China) in accordance with the manufacturer's protocol. After protein denaturation by boiling for 5 min, a 50 μg protein sample was loaded for separation on SDS-PAGE gel (BIO-RAD Co., California, USA). Proteins were transferred to PVDF membrane by wet-transfer process. The membrane was blocked in 5% non-fat milk powder or bovine serum albumin (BSA) (Sangon Biotech Inc., Shanghai, China) at room temperature for two h, and then incubated with primary antibodies at 4 °C overnight. After washing in TBST buffer (15 min $\times$ 3), the secondary antibody was applied at room temperature for one h. Antibodies bound to protein bands were detected by enhanced chemiluminescence (ECL) detection system. Band intensities were quantified using Image J software. GAPDH was used as the internal housekeeping control.

2.7 Statistical analysis

All data are shown as mean ± SEM (standard error of the mean). SPSS 22.0 software was used to analyze the correlation between groups by one-way ANOVA with the Tukey test. $P < 0.05$ was used as the threshold of statistical significance.

3. Results

3.1 Revolving rings number and left forelimb usage significantly declined after BAI treatment

As described previously, 6-OHDA-induced unilateral lesions to the substantia nigra cause asymmetric motor impairments, including reduced use of the contralateral forelimb and aberrant turning behavior, which can be monitored using rotation tests. Two weeks after modeling, the rats in NC group showed no turn behavior, while rats in the model group were observed to turn at more than seven cycles per minute. This finding indicated the successful establishment of the PD model. Compared with NC group, the number of the revolving ring was significantly increased in model group rats tested at 2 and 4 weeks ($P < 0.001$, respectively, Fig. 1). Remarkably, the revolving rings number was significantly reduced following 2 and 4 weeks of treatment in BAI-treated rats ($P < 0.001$, Fig. 1).

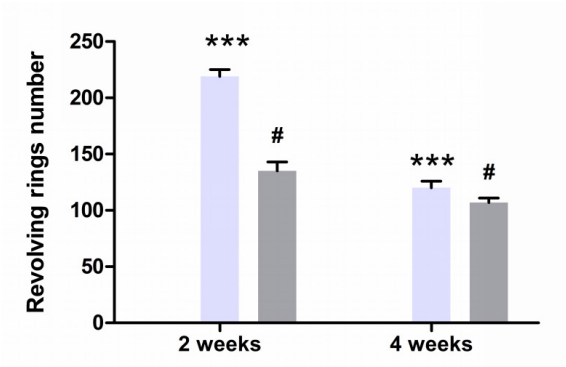

Figure 1. Number of revolving rings per treatment group. Data are expressed as mean ± SEM (n = 3). NC = normal control group; Model = model group; Treatment = BAI group. ***: $P < 0.001$, compared with NC group; #: $P < 0.001$, compared with model group (one-way ANOVA).

Four weeks after modeling, the rotation speed of rats in model group was significantly up-regulated, as compared to NC group ($P < 0.001$, Fig. 2). However, BAI group rats showed a significantly decreased rotation speed as compared with to model group ($P < 0.001$, Fig. 2). Finally, as shown by results from the cylinder experiment, left forelimb usage declined significantly in model group rats as compared to controls ($P < 0.001$, Fig. 2). However, BAI treatment resulted in significantly higher left forelimb usage when compared with the model group ($P < 0.001$, Fig. 2). Together, these results indicate that BAI treatment results in a significant recovery of functional motor impairments caused by 6-OHDA-induced PD in rats.

3.2 BAI treatment suppressed neuronal apoptosis

To ask whether 6-OHDA-induced lesions caused neuronal loss and if this loss was recovered by BAI treatment, TUNEL staining was performed on whole brain slices of rats from the three treatment groups. TUNEL-stained apoptotic neurons cells were detected as dark brown cells. As expected, the proportion of apoptotic cells was significantly enhanced in the brains of model group rats, indicating a higher rate of cell death ($P < 0.001$, Fig. 3). However, the rate of apoptotic cells was significantly suppressed in BAI-treated rats as compared to the model group ($P < 0.001$, Fig. 3). These results suggest that BAI is effective in suppressing neuronal apoptosis induced in PD brain tissue.

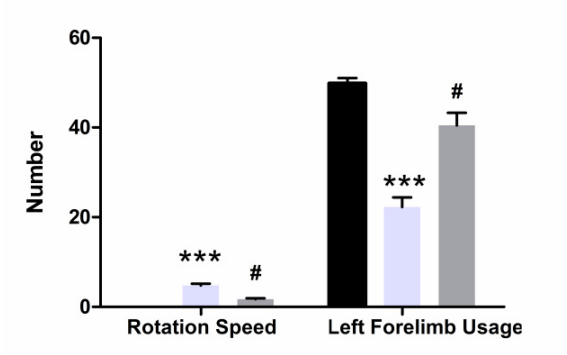

Figure 2. Measurement of rotation speed and left forelimb usage per treatment group. Data are expressed as mean ± SEM (n = 3). NC = normal control group. Model = model group. Treatment = BAI group. ***: $P < 0.001$, compared with NC group; #: $P < 0.001$, compared with model group (one-way ANOVA).

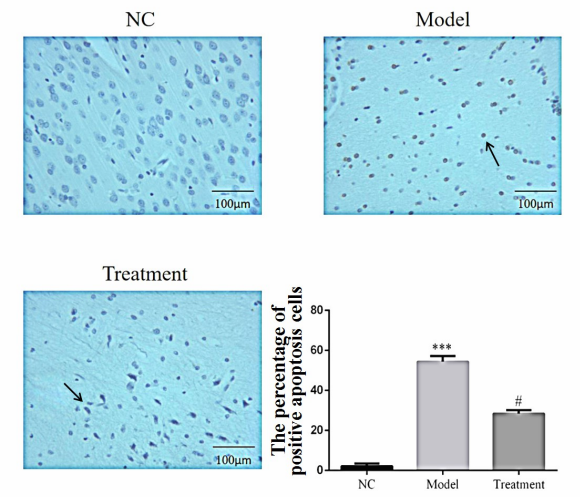

Figure 3. The percentage of TUNEL-positive apoptotic cells per group (× 200). Data are expressed as mean ± SEM (n = 3). NC = normal control group. Model = model group. Treatment = BAI group. ***: $P < 0.001$, compared with NC group; #: $P < 0.001$, compared with model group (one-way ANOVA).

3.3 BAI controls α-SYN expression in the substantia nigra

We next performed immunohistochemistry (IHC) staining to determine the expression pattern of α-synuclein (α-SYN). α-SYN protein was detected in neurons of the substantia nigra. Interestingly, while α-SYN expression was significantly enhanced in

model group rats as compared to the NC group ($P < 0.001$, Fig. 4), its expression was significantly suppressed in BAI group rats ($P < 0.001$, Fig. 4). These results showed that BAI could suppress α-SYN protein expression in PD model rats induced by 6-OHDA.

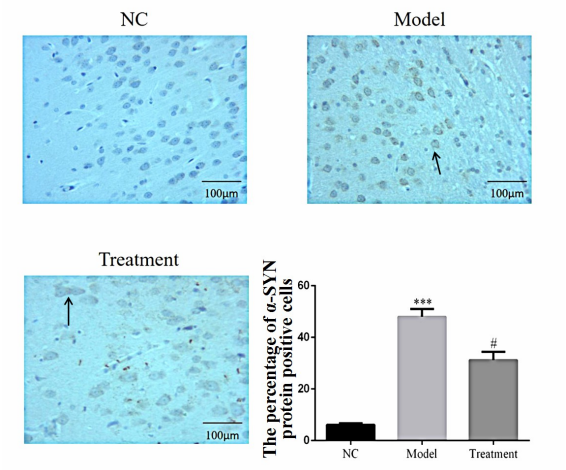

Figure 4. Percentage of α-SYN-positive cells per group detected by IHC ($\times$ 200). Data are expressed as mean $\pm$ SEM (n = 3). NC = normal control group. Model = model group. Treatment = BAI group. ***: $P < 0.001$, compared with NC group; #: $P < 0.001$, compared with model group (one-way ANOVA).

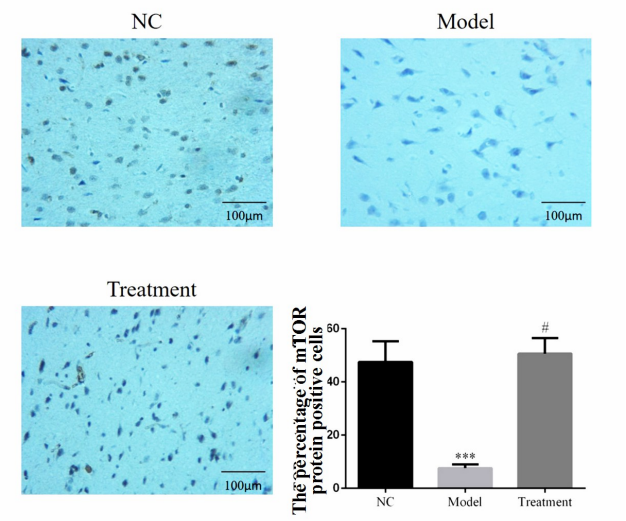

Figure 5. Percentage of mTOR-positive cells per group detected by IHC ($\times$ 200). Data are expressed as mean $\pm$ SEM (n = 3). NC = normal control group. Model = model group. Treatment = BAI group. ***: $P < 0.001$, compared with NC group; #: $P < 0.001$, compared with model group (one-way ANOVA).

3.4 BAI modulates mTOR/AKT/ GSK-3β signaling in PD model brains

Given the reported link between PD and mTOR/AKT/GSK-3β signaling and the known role of this pathway in cell apoptosis, we next examined the expression levels of these proteins. The expression of mTOR, p-mTOR, AKT, p-AKT, GSK-3β, and p-GSK-3β was visualized in rat brain sections using IHC. Intriguingly, protein expression was strongly reduced in model group rats compared to NC rats ($P < 0.001$, respectively, Fig. 5-10). However, BAI treatment caused a significant increase in protein expression as compared to the model group ($P < 0.001$, respectively, Fig. 5-10).

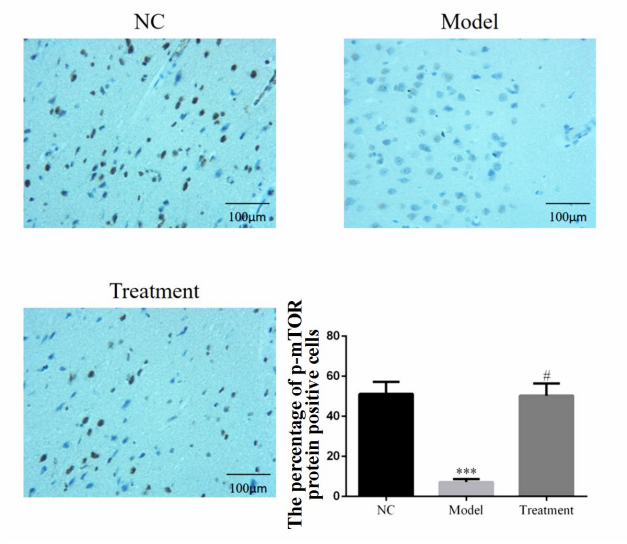

Figure 6. Percentage of p-mTOR-positive cells per group detected by IHC ($\times$ 200). Data are expressed as mean $\pm$ SEM (n = 3). NC = normal control group. Model = model group. Treatment = BAI group. ***: $P < 0.001$, compared with NC group; #: $P < 0.001$, compared with model group (one-way ANOVA).

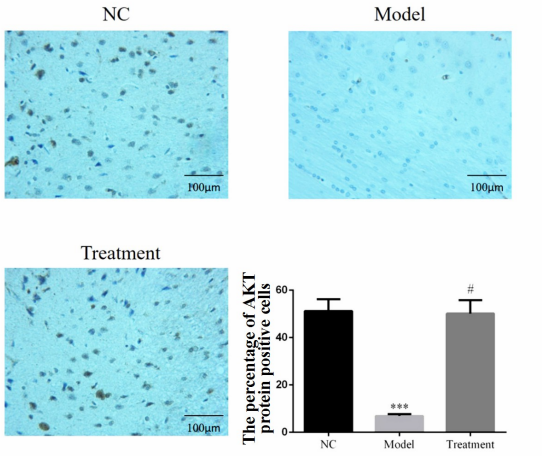

Figure 7. Percentage of AKT-positive cells per group detected by IHC ($\times$ 200). Data are expressed as mean $\pm$ SEM (n = 3). NC = normal control group. Model = model group. Treatment = BAI group. ***: $P < 0.001$, compared with NC group; #: $P < 0.001$, compared with model group (one-way ANOVA).

These results were further confirmed by Western blot measurements on brain tissue. Protein expression of mTOR, p-mTOR, AKT, p-AKT, GSK-3β, and p-GSK-3β was significantly down-regulated in the model group versus NC control rats ($P < 0.001$,

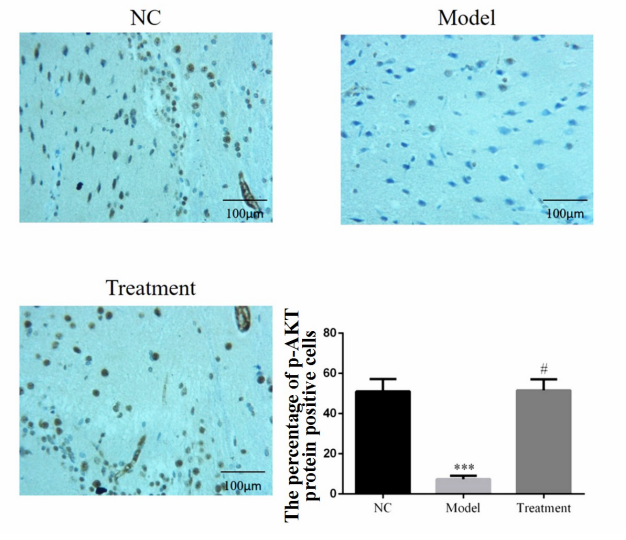

Figure 8. Percentage of p-AKT-positive cells per group detected by IHC (× 200). Data are expressed as mean ± SEM (n = 3). NC = normal control group. Model = model group. Treatment = BAI group. ***: $P < 0.001$, compared with NC group; #: $P < 0.001$, compared with model group (one-way ANOVA).

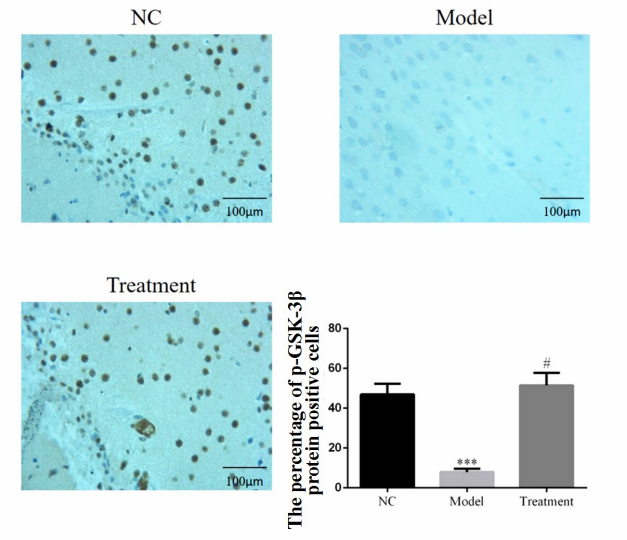

Figure 10. Percentage of p-GSK-3β-positive cells per group detected by IHC (× 200). Data have expressed a means ± SEM (n = 3). NC = normal control group. Model = model group. Treatment = BAI group. ***: $P < 0.001$, compared with NC group; #: $P < 0.001$, compared with model group (one-way ANOVA).

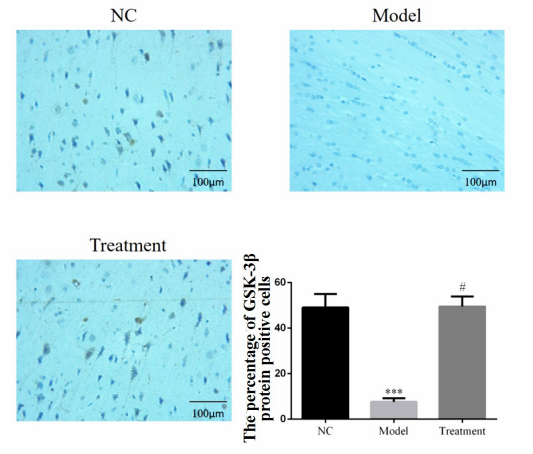

Figure 9. Percentage of GSK-3β protein-positive cells in different groups detected by IHC assay (× 200). Data were expressed as means ± SEM (n = 3). NC was normal control group. The model was model group. Treatment was BAI group. ***: $P < 0.001$, compared with NC group; #: $P < 0.001$, compared with model group (one-way ANOVA).

respectively, Fig. 11). However, the expression of all proteins was significantly enhanced in BAI-treated versus model group rats ($P < 0.001$, respectively, Fig. 11). Together, these results illustrate that changes in mTOR/AKT/GSK-3β signaling in PD model rats were strongly recovered by BAI treatment.

4. Discussion

Parkinson's disease (PD) is a common neurodegenerative disease in middle and old age. The pathogenesis of PD is closely related to immune inflammation, oxidative stress, excitatory neurotoxicity, and heredity/environment (Cramer et al., 2012). The main pathological feature of PD was nigrostriatal lesion. In present study, we established PD rat model by intraperitoneal injection of 6-OHDA to evaluate the effect of BAI on substantia nigra neuronal apoptosis. The results showed that the left forelimb use rate was significantly reduced in rats induced with 6-OHDA, which was significantly increased by BAI treatment. It suggested that the PD rat model was successfully established.

BAI, along with its metabolite baicalein have many targets and may have protective effects on diverse diseases. The previous studies found that BAI had effects on neuroprotective, renovascular hypertension, cancer, obesity, and liver dysfunction (Dai et al., 2017; Sowndhararajan et al., 2018; Tang et al., 2016; Xi et al., 2015). However, it has been unclear that the effects and mechanisms of BAI on PD treatment. The massive loss of dopamine neurons in the substantia nigra is a major pathological change in the pathogenesis of PD (Ariza et al., 2015). There were many eosinophilic inclusion bodies (Lewy body, LBs) in neuronal cytoplasm, and the main component of LBs was α-synuclein (α-SYN) (Mollenhauer et al., 2012). α-SYN over-expression could induced dopamine neurons die by vesicle permeability-increasing and Ca^{2+} internal flowing (Kalia and Kalia, 2015). These results suggested that α-SYN expression also indirectly reflected the reduction of dopamine neurons. In our present study, the results indicated that the nerve cell apoptosis rate in model group was significantly increased when compared with that in NC group. However, the cell apoptosis rate in BAI group was significantly suppressed with BAI treatment when compared with that in model group. Those results showed that BAI had effects on improving nerve cell apoptosis induced by PD.

There were some reports that the activation of mTOR/AKT/GSK-3β pathway could have protective effects on neuronal apoptosis induced by 6-OHDA (Armentero et al., 2011; Ding et al., 2017). In our present study, we found that the

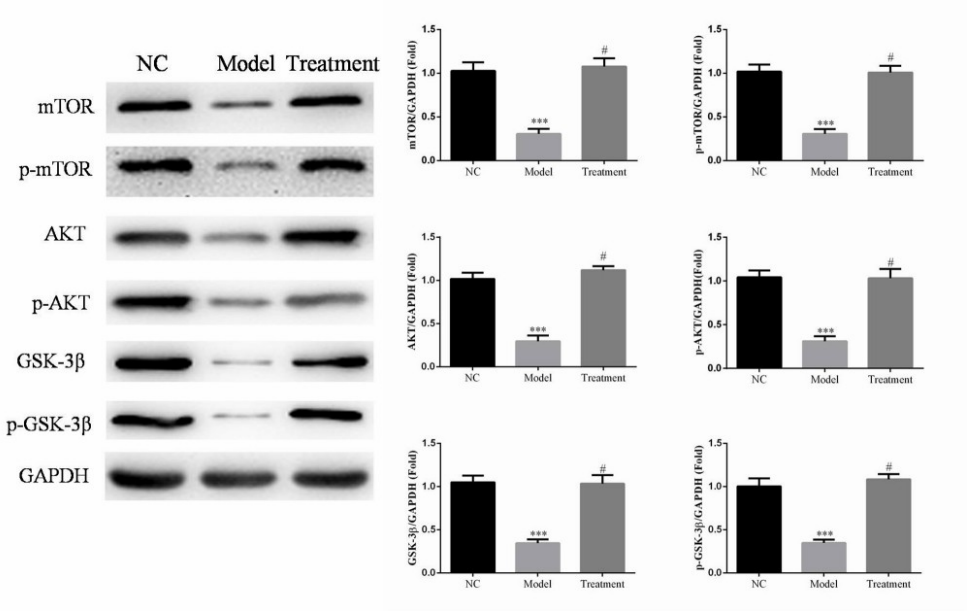

Figure 11. Protein expressions of mTOR, p-mTOR, AKT, p-AKT, GSK-3β, and p-GSK-3β compared between treatment groups by western blot. Band intensities were normalized to GAPDH and expressed as relative values. Data are expressed as means ± SEM (n = 3). NC = normal control group. Model = model group. Treatment = BAI group. ***: $P < 0.001$, compared with NC group; #: $P < 0.001$, compared with model group (one-way ANOVA).

protein expression levels of mTOR, p-mTOR, AKT, p-AKT, GSK-3β, and p-GSK-3β were significantly decreased in rats induced by 6-OHDA when compared with control group. The results showed that the inhibition of mTOR/AKT/GSK-3β pathway was closely correlation with nerve cell apoptosis induced by PD. It is reported that baicalin attenuates ketamine-induced neurotoxicity in the developing rats via PI3K/Akt and CREB/BDNF/Bcl-2 pathways (Zuo et al., 2016). Furthermore, BAI had effects of anti-mycobacterial and anti-inflammatory through inhibiting the PI3K/Akt/NF-κB pathway (Zhang et al., 2017). Besides, Baicalin ameliorates neuroinflammation-induced depressive-like behavior through inhibition of toll-like receptor four expressions via the PI3K/AKT/FoxO1 pathway (Guo et al., 2019). Our results showed that BAI treatment could significantly suppress the cell apoptosis rate in PD rats, and the mechanism might be correlation with the activation of mTOR/ AKT/GSK-3β pathway.

In conclusion, our results suggested that BAI has a protective effect on improving substantia nigra neurons apoptosis in PD rats by directly regulating the mTOR/AKT/GSK-3β pathway.

Acknowledgment

The comments of two anonymous reviewers improved our first draft.

Conflict of interest

The authors declare no conflict of interest.

Submitted: June 27, 2019
Accepted: August 22, 2019
Published: December 30, 2019

References

Ariza, D., Lopes, F. N. C., Crestani, C. C. and Martins-Pinge, M. C. (2015) Chemoreflex and baroreflex alterations in Parkinsonism induced by 6-OHDA in unanesthetized rats. *Neuroscience Letters* **607**, 77-82.

Armentero, M. T., Sinforiani, E., Ghezzi, C., Bazzini, E., Levandis, G., Ambrosi, G., Zangaglia, R., Pacchetti, C., Cereda, C., Cova, E., Basso, E., Celi, D., Martignoni, E., Nappi, G. and Blandini, F. (2011) Peripheral expression of key regulatory kinases in Alzheimer's disease and Parkinson's disease. *Neurobiology Aging* **32**, 2142-2151.

Chung, J. Y, Lee, S. J., Lee, S. H., Jung, Y. S., Ha, N. C., Seol, W. and Park, B. J. (2011) Direct interaction of α-synuclein and AKT regulates IGF-1 signaling: implication of Parkinson disease. *Neurosignals* **19**, 86-96.

Cramer, P. E., Cirrito, J. R., Wesson, D. W., Lee, C. Y., Karlo, J. C., Zinn, A. E., Casali, B. T., Restivo, J. L., Goebel, W. D., James, M. J., Brunden, K. R., Wilson, D. A. and Landreth, G. E. (2012) ApoE-directed therapeutics rapidly clear β-amyloid and reverse deficits in AD mouse models. *Science* **335**, 1503-1506.

Dai, H., Zhang, X., Yang, Z., Li, J. and Zheng, J. (2017) Effects of baicalin on blood pressure and left ventricular remodeling in rats with renovascular hypertension. *Medical Science Monitor* **23**, 2939-2948.

Deng, H., Wang, P. and Jankovic, J. (2017) The genetics of Parkinson's disease. *Ageing Research Reviews* **42**, 72-85.

Ding, M. L., Ma, H., Man, Y. G. and Lv, H. Y. (2017) Protective effects of a green tea polyphenol, epigallocatechin-3-gallate, against sevoflurane-induced neuronal apoptosis involve regulation of CREB/BDNF/TrkB and PI3K/Akt/mTOR signalling pathways in neonatal mice. *Canadian Journal of Physiology and Pharmacology* **95**, 1396-1405.

Guo, L. T., Wang, S. Q., Su, J., Xu, L. X., Ji, Z. Y., Zhang, R. Y., Zhao, Q. W., Ma, Z. Q., Deng, X. Y. and Ma, S. P. (2019) Baicalin ameliorates neuroinflammation-induced depressive-like behavior through inhibition of toll-like receptor 4 expression via the PI3K/AKT/FoxO1 pathway. *Journal of Neuroinflammation* **16**, 95.

Heras-Sandoval, D., Pérez-Rojas, J. M., Hernández-Damián, J. and Pedraza-Chaverri, J. (2014) The role of PI3K/AKT/mTOR pathway in the modulation of autophagy and the clearance of protein aggregates in neurodegeneration. *Cell Signal* **26**, 2694-2701.

Huang, J., Liu, W., Doycheva, D. M., Gamdzyk, M., Lu, W., Tang, J. and Zhang, J. H. (2019) Ghrelin attenuates oxidative stress and neuronal apoptosis via GHSR-1α/AMPK/Sirt1/PGC-1α/UCP2 pathway in a rat model of neonatal HIE. *Free Radical Biology & Medicine* **141**, 322-337.

Jiang, W. B., Zhao, W., Chen, H., Wu, Y. Y., Wang, Y., Fu, G. S. and Yang, X. J. (2018) Baicalin protects H9c2 cardiomyocytes against hypoxia/reoxygenation-induced apoptosis and oxidative stress through activation of mitochondrial aldehyde dehydrogenase 2. *Clinical and Experimental Pharmacology and Physiology* **45**, 303-311.

Kalia, L. V. and Kalia, S. K. (2015) α-Synuclein and Lewy pathology in Parkinson's disease. *Current Opinion in Neurology* **28**, 375-381.

Khwanraj, K., Madlah, S., Grataitong, K. and Dharmasaroja, P. (2016) Comparative mRNA expression of eEF1A isoforms and a PI3K/AKT/mTOR pathway in a cellular model of Parkinson's disease. *Parkinsons Disease* **2016**, 8716016.

Konnova, E. A., Swanberg, M., Stoker, T. B. and Greenland, J. C. (2018) Parkinson's disease: pathogenesis and clinical aspects. *Brisbane (AU): Codon Publications*.

Lazzarini, M., Martin, S., Mitkovski, M., Vozari, R. R., Stühmer, W. and Bel, E. D. (2013) Doxycycline restrams glia and confers neuroprotection in a 6-OHDA Parkinson model. *Glia* **61**, 1084-1100.

Li, X., Zou, K., Gou, J., Du, Q., Li, D., He, X. and Li, Z. (2015) Effect of baicalin-copper on the induction of apoptosis in human hepatoblastoma cancer HepG2 cells. *Medical Oncology* **32**, 72.

Manohar, S. G. and Husain, M. (2015) Reduced papillary reward sensitivity in Parkinson's disease. *Parkinson Disease* **1**, 15026.

Mollenhauer, B., Trautmann, E., Otte, B., Ng, J., Spreer, A., Lange, P., Sixel-Döring, F., Hakimi, M., Vonsattel, J. P., Nussbaum, R., Trenkwalder, C. and Schlossmacher, M. G. (2012) α-Synuclein in human cerebrospinal fluid is principally derived from neurons of the central nervous system. *Journal of Neural Transmission* **119**, 739-746.

Morales-García, J. A., Susín, C., Alonso-Gil, S., Pérez, D. I., Palomo, V., Pérez, C., Conde, S., Santos, A., Gil, C., Martínez, A. and Pérez-Castillo, A. (2013) Glycogen synthase Kinase-3 inhibitors as potent therapeutic agents for the treatment of Parkinson disease. *ACS Chemical Neuroscience* **4**, 350-360.

Prusiner, S. B., Woerman, A. L., Mordes, D. A., Watts, J. C., Rampersaud, R., Berry, D. B., Patel, S., Oehler, A., Lowe, J. K., Kravitz, S. N., Geschwind, D. H., Glidden, D. V., Halliday, G. M., Middleton, L. T., Gentleman, S. M., Grinberg, L. T. and Giles, K. (2015) Evidence for α-synuclein prions causing multiple system atrophy in humans with parkinsonism. *Proceedings of the National Academy of Sciences of the United States of America* **112**, E5308-5317.

Radder, D. L. M., Sturkenboom, I. H., van Nimwegen, M., Keus, S. H., Bloem, B. R. and de Vries, N. M. (2017) Physical therapy and occupational therapy in Parkinson's disease. *International Journal of Neuroscience* **127**, 930-943

Sadowski, K., Kotulska-Jóźwiak, K. and Jóźwiak, S. (2015) Role of mTOR inhibitors in epilepsy treatment. *Pharmacological Reports* **67**, 636-646.

Saxena, C. C., Safaya, R., Kawatra Madan, N., Khan, S. A. and Iyer, V. K. (2016) Histopathological, immunohistochemical, and image analytic parameters characterizing the stromal component in primary and recurrent giant cell tumor of bone. *Journal of Clinical Orthopaedics and Trauma* **7**, 109-114.

Schallert, T., Fleming, S. M., Leasure, J. L., Tillerson, J. L. and Bland, S. T. (2000) CNS plasticity and assessment of forelimb sensorimotor outcome in unilateral rat models of stroke, cortical ablation, parkinsonism and spinal cord injury. *Neuropharmacology* **39**, 777-787.

Schwarting, R. K., Bonatz, A. E., Carey, R. J. and Huston, J. P. (1991) Relationships between indices of behavioral asymmetries and neurochemical changes following mesencephalic 6-hydroxydopamine injections. *Brain Research* **554**, 46-55.

Shou, X., Wang, B., Zhou, R., Wang, L., Ren, A., Xin, S. and Zhu, L. (2017) Baicalin Suppresses Hypoxia-Reoxygenation-Induced Arterial Endothelial Cell Apoptosis via Suppressing PKCδ/p53 Signaling. *Medical Science Monitor* **23**, 6057-6063.

Sun, G., Xing, C., Zeng, L., Huang, Y., Sun, X. and Liu, Y. (2019) Flemingia philippinensis Flavonoids Relieve Bone Erosion and Inflammatory Mediators in CIA Mice by Downregulating NF-κB and MAPK Pathways. *Mediators of Inflammation* **2019**, 5790291.

Sowndhararajan, K., Deepa, P., Kim, M., Park, S. J. and Kim, S. (2018) Neuroprotective and cognitive enhancement potentials of baicalin: a review. *Brain Sciences* **8**, E104.

Tan, H. Y., Wang, N., Man, K., Tsao, S. W., Che, C. M. and Feng, Y. (2012) Autophagy-induced RelB/p52 activation mediates tumour-associated macrophage repolarisation and suppression of hepatocellular carcinoma by natural compound baicalin. *Cell Death & Disease* **6**, e1942.

Tang, Q., Ji, F., Sun, W., Wang, J., Guo, J., Guo, L., Li, Y. and Bao, Y. (2016) Combination of baicalein and 10-hydroxy camptothecin exerts remarkable synergetic anti-cancer effects. *Phytomedicine* **23**, 1778-1786.

Tang, S., Wang, A., Yan, X., Chu, L., Yang, X., Song, Y., Sun, K., Yu, X., Liu, R., Wu, Z. and Xue, P. (2017) Brain-targeted intranasal delivery of dopamine with borneol and lactoferrin co-modified nanoparticles for treating Parkinson's disease. *Drug Delivery* **26**, 700-707.

Thiele, S. L., Warre, R. and Nash, J. E. (2012) Development of a unilaterally-lesioned 6-OHDA mouse model of Parkinson's disease. *Journal Visualized Experiments* **60**, 3234.

Yang, S., Fu, Y., Wu, X., Zhou, Z., Xu, J., Zeng, X., Kuang, N. and Zeng, Y. (2014) Baicalin prevents Candida albicans infections via increasing its apoptosis rate. *Biochemical and Biophysical Research Communications* **451**, 36-41.

Xi, Y., Wu, M., Li, H., Dong, S., Luo, E., Gu, M., Shen, X., Jiang, Y., Liu, Y. and Liu, H. (2015) Baicalin attenuates high fat diet-induced obesity and liver dysfunction: dose-response and potential role of CaMKKβ/AMPK/ACC pathway. *Cellular Physiology and Biochemistry* **35**, 2349-2359.

Zuo, D., Lin, L., Liu, Y., Wang, C., Xu, J., Sun, F., Li, L., Li, Z. and Wu, Y. (2016) Baicalin attenuates ketamine-induced neurotoxicity in the developing rats: involvement of PI3K/Akt and CREB/BDNF/Bcl-2 pathways. *Neurotoxicity Research* **30**, 159-172.

Zhang, Q., Sun, J., Wang, Y., He, W., Wang, L., Zheng, Y., Wu, J., Zhang, Y. and Jiang, X. (2017) Antimycobacterial and Anti-inflammatory Mechanisms of Baicalin via Induced Autophagy in Macrophages Infected with Mycobacterium tuberculosis. *Frontiers in Microbiology* **8**, 2412.